Table 1 Results of sample numerical calculation

	Subsonic (region I)	Supersonic (region II)
N	1.155	0.180
C_{DL}	2.910	0.313
C_{DLeff}	0.752	0.270
C_D	10	7.5 (with centrifugal correction)
% increase in drag caused by MADD:		
C_{DLeff}/C_D = 10.2% (both regions considered)		= 13.6% (with centrifugal correction)
C_{DLeff}/C_D = 7.5% (subsonic only)		= 10.0% (with centrifugal correction)

The hypersonic drag coefficient based on simple impact theory is found from Ref. 6 to be $C_D = 1$ based on the area πR^2 with no centrifugal effect correction and $C_D = 0.75$ with centrifugal correction. This is at zero angle of attack. However, in the preceding analysis, the C_{DL}'s are based on a different area so that $C_D = R/\delta R$ based on that different area. With centrifugal correction $C_D = 0.75\ R/\delta R$. A numerical example for $R = 1m$, $\delta R = 0.1$m, and the values for the various constants, as shown in the figures, is given in Table 1. In Fig. 4, this result is compared with experimental results from Ref. 1.

Discussion and Results

Even though many assumptions have been made and the actual problem of hypersonic flow around a blunt body with a magnetic field internally generated appears to be almost obscured, it is felt that this method has merit in yielding qualitative answers. It is safe to assume that, in the flight range during re-entry where the conductivity is sufficiently high, drag will increase between 7 and 14% (see Ref. 7 for an estimate of magnetohydrodynamic flight ranges). Whether this is large enough to merit using MADD is a problem left for the vehicle designer.

Some of the inaccuracies in the method include the assumption of a constant radial magnetic field. The field of a real magnet would decrease inversely with the radius and directly with the angle θ. The assumption of the streamtube with constant area needs no further discussion, since it is clearly just a first-order approximation used to make the approach possible. The location of a sonic line at $\theta = 30°$ does not account for sonic line shift, and thus, the lengths used for each region are not exact. The supersonic region gives considerably smaller results, which are open to question and could be ignored without altering the over-all results much. We have not given any consideration to the shape of the shock wave or to the effect of the $\mathbf{J} \times \mathbf{B}$ force on the shock standoff distance. The standoff distance was not used as the characteristic length in N. In conclusion, this note has been written to show a method of computation which is simple enough for the slide rule and which gives qualitative results for a rather complex problem.

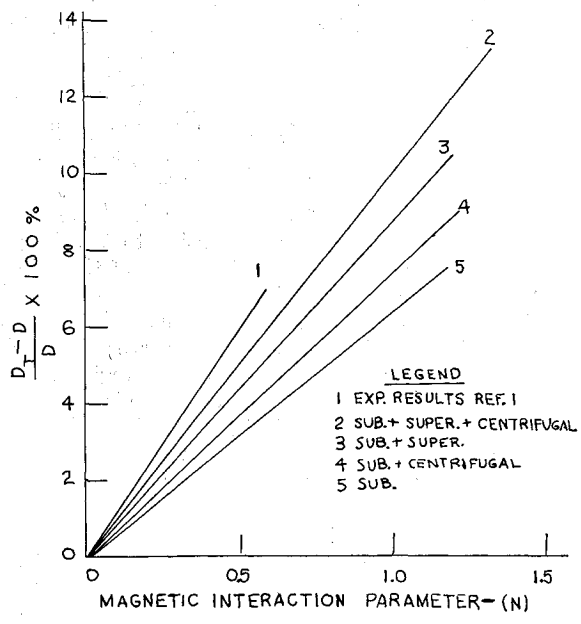

Fig. 4 Comparison of experimental results of Ref. 1 with the results of this analysis.

References

[1] Seemann, G. R., "Experimental aspects of magnetoaerodynamic drag," Ph.D. Dissertation, Gas Dynamics Lab., Northwestern Univ. (1964).

[2] Ericson, W. B. and Maciulaitis, A., "Investigation of magnetohydrodynamic flight control," J. Spacecraft Rockets 1, 283–289 (1964).

[3] Heims, S. P., "Effects of oxygen recombination in one-dimensional flow at high Mach numbers," NACA-TN 4144 (1958).

[4] Bray, K. N. C. and Wilson, J. A., "A preliminary study of ionic recombination of argon in a wind tunnel nozzle," Univ. of Southampton, Southampton, England, Rept. AASU 134 (1960).

[5] Bray, K. N. C. and Wilson, J. A., "A preliminary study of ionic recombination of argon in wind tunnel nozzles Part II," Univ. of Southampton, Southampton, England, Rept. AASU 185 (1960).

[6] Truitt, R. W., *Hypersonic Aerodynamics* (Ronald Press Company, New York, 1959), Chap. 1, p. 11.

[7] Kantrowitz, A., "Flight magnetohydrodynamics," *Symposium of Plasma Dynamics*, edited by F. H. Clauser (Addison-Wesley Publishing Co., Inc., Reading, Mass., 1960), Chap. VII.

Closed-Loop Simulation of Inertial Platform Accelerometer Inputs

F. F. Schloetzer* and C. T. Jackson Jr.†
Martin Company, Orlando, Fla.

THE highly successful flight-test program for the Army's Pershing ballistic missile climaxed an ambitious preflight system testing effort. Through analog simulations, the missile system was preflight certified, the design was validated, and system performance was evaluated. A basic objective of such simulations is to include a maximum of flight hardware in the tests. This note describes a technique that permits closed-loop operation (Fig. 1) of the complete guidance system by simulating acceleration from lift-off to end of powered flight through the use of programed torquers on the input axes of the inertial-platform accelerometers. Closed-loop operation of the inertial guidance system (Fig. 1) obviates many shortcomings in system evaluation. Manual loading or programing of guidance-system errors and trajectory data is avoided. Without loop closure, any test is merely an autopilot simulation that neglects vital test parameters. Torquers of the type described herein are now used in all analog flight simulation studies of the Pershing missile.

Torque Design

The design requirements for the torquer were as follows: 1) generate linear inputs simulating accelerations up to $\pm 3g$; 2) be adaptable to existing accelerometer hardware, i.e., any insertion device must operate within the enclosed cup of the accelerometer; 3) be excitable from programed

Received August 17, 1964; revision received May 20, 1965.
* Associate Research Scientist.
† Design Specialist.

amplifiers limited to 85-v output; 4) cause no change in precession constant or side balance of the accelerometer; and 5) contribute no residual or constant torque.

A torquing unit using a polarized solenoid was tried first. It met most of the requirements and proved the feasibility of the concept, but it had residual torques that required cancellation through electrical biasing. The design subsequently adopted (Fig. 2) met all of the requirements and eliminated the biasing problem. An important feature is the extended active length of the coil. The torquer unit was designed to use all of the available space on the mass balance end of the air bearing cylinder. The four-coil, four-magnet-cup unit provides the symmetry necessary to keep the inner cylinder balanced. The arrangement in two pairs of back-to-back magnet cups enhances the keeper quality of the steel cups and provides for very accurate calibration, because the number of active turns remains constant as the magnets move into and away from the coil bobbins during the small rotational movements of the inner cylinder; the magnets move toward two of the layer-wound coils as they move away from the remaining two. Polarized magnets allow all of the coils to be active during either positive or negative rotation of the accelerometer measuring head.

The precession (output) of an integrating accelerometer results from a torque T on its input axis which follows the gyro law $T = \omega H$. The simulated torque per g of acceleration (T/g, g-cm) is provided by the force and moment arm of the magnet-coil assembly as follows:

$$T/g = \omega H/g = fl = (10^{-7}\,\beta LI/g)l \qquad (1)$$

where g = gravitational acceleration, 980 cm/sec^2; ω = precession rate, rad/sec; H = angular momentum of wheel g-cm^2/sec; f = force, g; l = moment arm, cm; the constant 10^{-7} results from the units chosen for β, L, and I; β = flux density, gauss; L = active wire length, cm; and I = current, ma.

For this particular accelerometer, $H = 1.15 \times 10^5$ g-cm^2/sec, and a 1-g input causes precession at 0.210 rad/sec, so that $T/g = 24.6$ g-cm, or 6.15 g-cm for each of the four magnet cups. The size of the nylon coil bobbin and the coil wire were governed by available space and slip-ring current limitations. The design chosen uses 324 active turns of number 42 wire on a mean coil diameter of 0.762 cm, giving L = 775 cm/coil. The moment arm l is 1.6 cm. If it is assumed that β = 800 gauss, then by Eq. (1) $I = 6.15\text{g}/10^{-7}$ (800) (775)(1.6) = 61 ma. In practice, more current than this was required, hence the flux density was somewhat less than 800 gauss for the magnet material used.

The four magnets are charged to saturation as an assembly and are subject to the sustained keeper action of the steel cups. The stray magnetic field problem, although greatly reduced by the magnet-cup configuration, still must be considered. All parts of the coil assembly must be entirely nonmagnetic. (One of the original wiring terminals appeared to be tinned copper but had a very slight magnetic property, which was not detected until the unit demonstrated a residual torque during preliminary testing.)

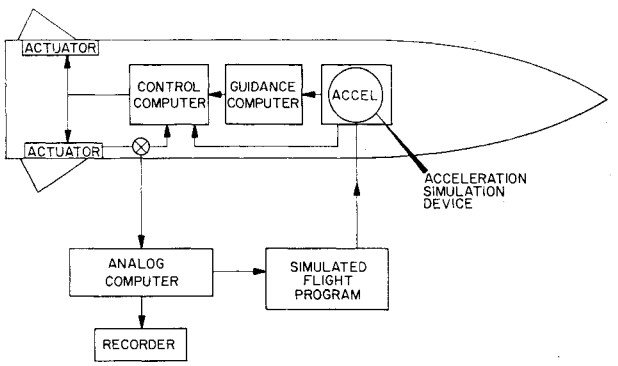

Fig. 1. Loop completion.

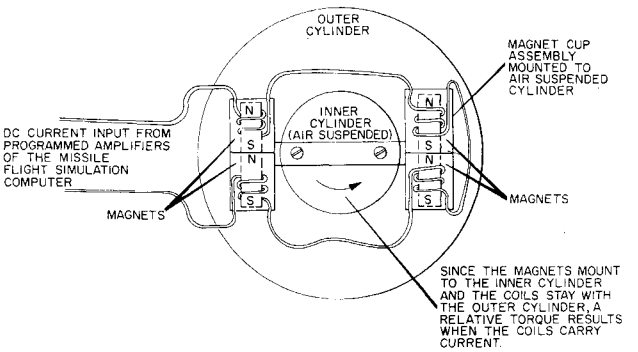

Fig. 2. Torquer configuration.

Calibration

For accelerations up to 1g, calibration of the torquer was accomplished by coupling accurate fractional components of the local gravity vector into the sensitive axis of the accelerometer and applying current to the torquer to cancel the resulting precession rate. For accelerations from 1 to 3g, the torquer was used to drive out the existing 1-g value and to generate an opposite precession rate equal to various g increments. All of this calibration was accomplished with the readout instrumentation already available for the accelerometer.

Stability of Constant-Altitude Re-Entry Flight Paths

ALLEN R. STUBBERUD*
University of California, Los Angeles, Calif.

ONE method of guidance of lifting bodies entering the earth's atmosphere at superorbital velocities is flight-path control, that is, the controlling of the body to fly a prechosen nominal flight path or trajectory.[1] A total re-entry trajectory is generally obtained by piecing together several simple trajectories such as constant-altitude or equilibrium-glide trajectories.[2] A question of concern in the method of flight-path control is that of the stability of the trajectory, that is, the property of the trajectory which determines whether or not the lifting body returns to the nominal trajectory without the application of control command whenever it is perturbed from the trajectory. In this note the stability of the class of constant-altitude trajectories is examined.

Velocity as the Independent Variable

The motion of the center of gravity of a lifting body entering the earth's atmosphere under the assumptions that 1) the earth is spherical and nonrotating; 2) the atmospheric density is exponential ($\rho = \rho_0 e^{-\beta h}$); and 3) the motion of the body is planar, is described by the set of equations

$$V\dot{\gamma} = -L/m - (V^2/r)\cos\gamma + g\cos\gamma \qquad (1)$$

$$\dot{V} = -D/m + g\sin\gamma \qquad (2)$$

$$\dot{\rho} = \beta V\rho\sin\gamma \qquad (3)$$

Received October 16, 1964; revision received March 19, 1965.
* Assistant Professor, Department of Engineering.